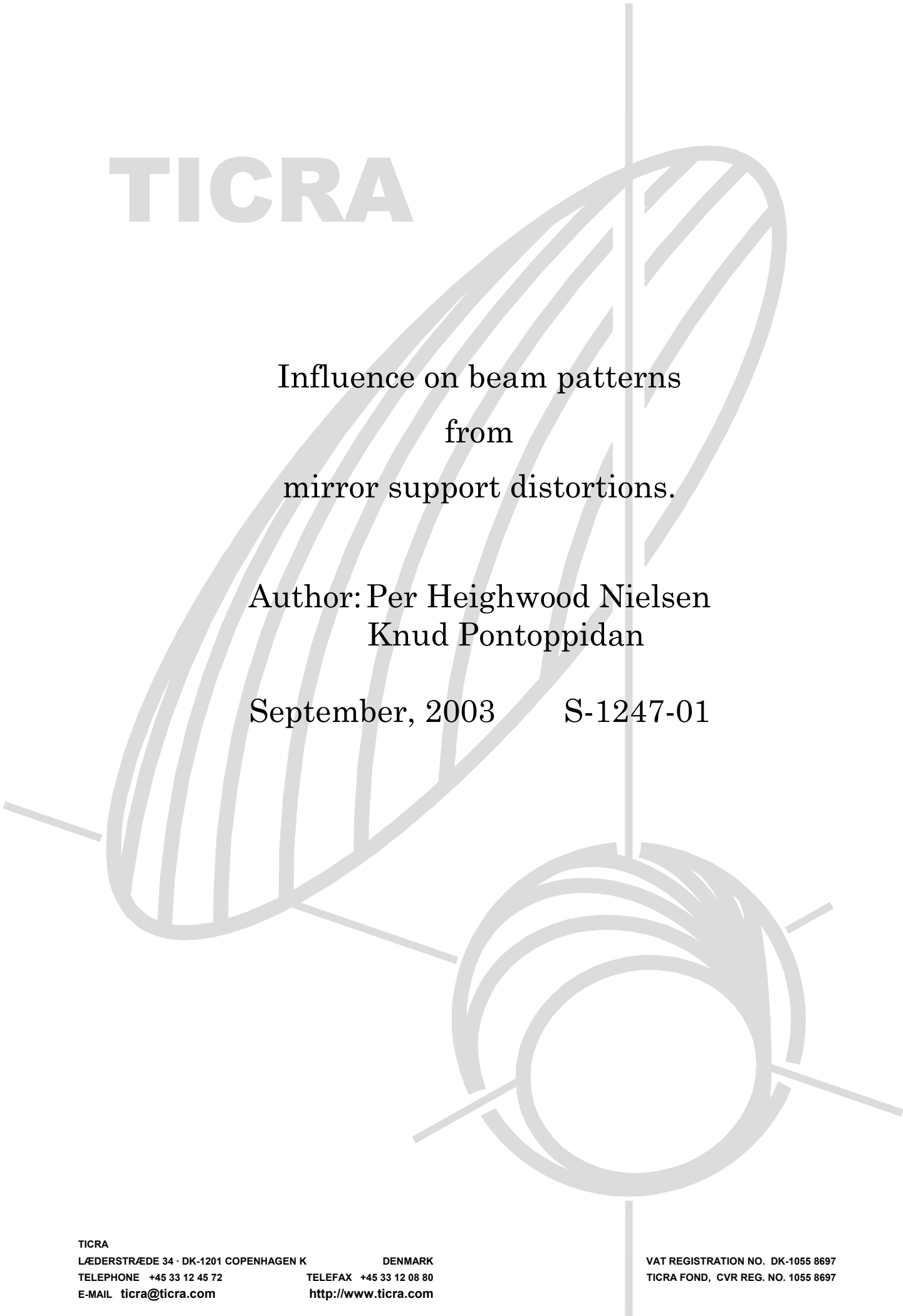


# TICRA



Influence on beam patterns  
from  
mirror support distortions.

Author: Per Heighwood Nielsen  
Knud Pontoppidan

September, 2003

S-1247-01

TICRA

LÆDERSTRÆDE 34 · DK-1201 COPENHAGEN K

DENMARK

TELEPHONE +45 33 12 45 72

TELEFAX +45 33 12 08 80

E-MAIL [ticra@ticra.com](mailto:ticra@ticra.com)

<http://www.ticra.com>

VAT REGISTRATION NO. DK-1055 8697

TICRA FOND, CVR REG. NO. 1055 8697



# PLANCK MIRROR SYSTEM

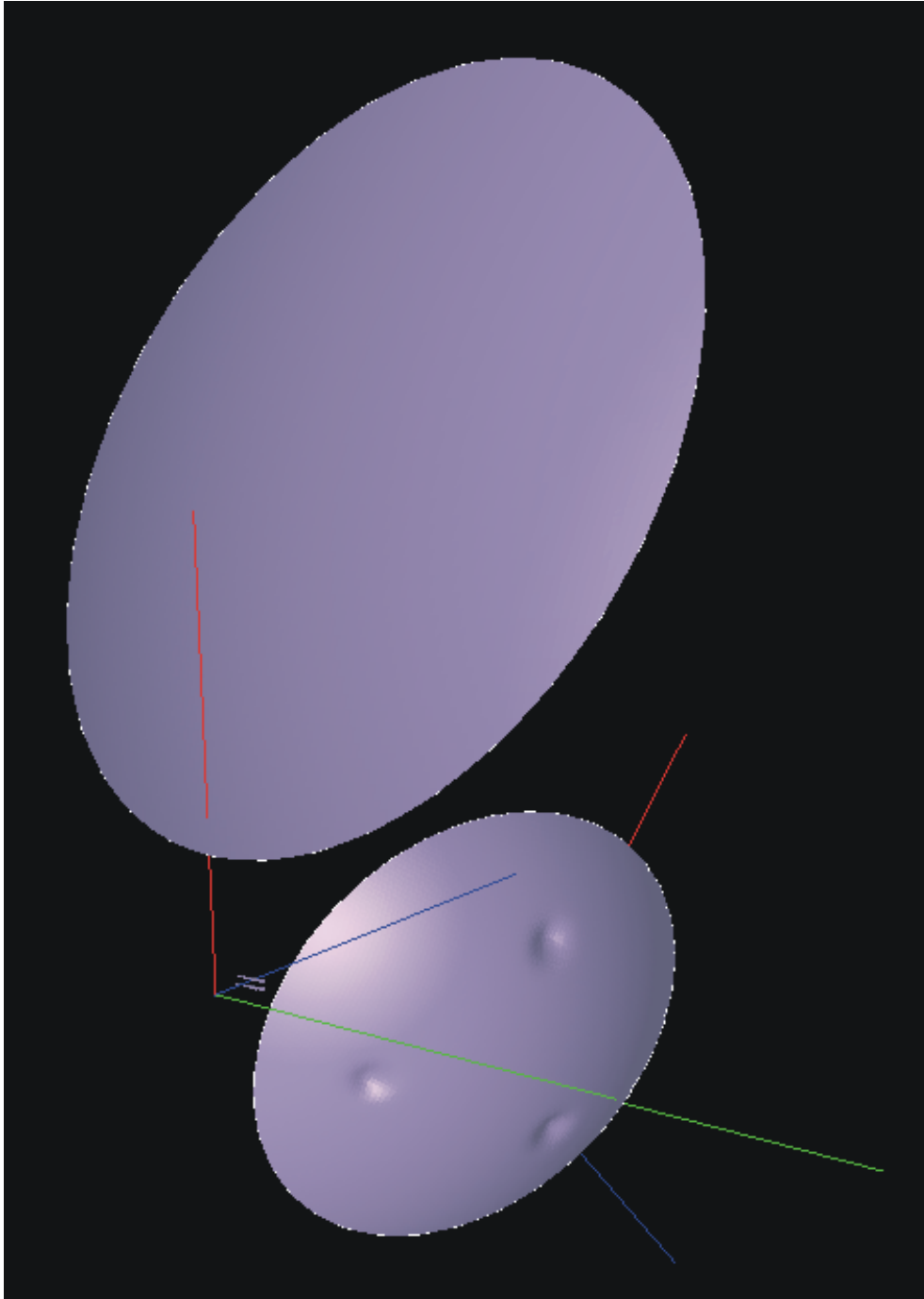


## TABLE OF CONTENTS

1. INTRODUCTION	1
2. SURFACE DISTORTION MODEL	2
3. RF DEGRADATION FOR 217 GHZ DETECTORS	3
3.1 HFI_217_01	4
3.2 HFI_217_02	7
3.3 HFI_217_05	10
3.4 HFI_217_06	13
4. SCALE INFLUENCE ON PERFORMANCE	16
REFERENCES	18

## 1. INTRODUCTION

The secondary mirror for the PLANCK telescope has now been manufactured and the surface accuracy has been measured. The measurement has been carried out using an ordinary 3D measuring machine at room temperature and the result shows that the accuracy is well within the required tolerances.

In the near future the mirror will also be measured at the operating temperature which is around 50° K. At this temperature another measurement technique must be used based on interferometry. It turns out, however, that in some areas of the mirror the measurement will fail due to too a high surface slope and this is likely to happen near the three mirror support points.

It is therefore of interest to investigate if a possible distortion at the support points might jeopardize the performance of the telescope.

The surface distortion has been modelled as simple Gaussian hats at each of the 3 support points as described in Chapter 2. The resulting influence on the beam patterns is investigated in Chapter 3 using four differently positioned detectors at 217 GHz. The RF dependence of the distortion peak scale is investigated in Chapter 4.

## 2. SURFACE DISTORTION MODEL

It has been decided to model the possible surface distortion near the support points as a Gaussian distribution with a maximum of  $20 \mu\text{m}$  and a standard deviation of  $30 \text{mm}$ . The distortion can then be expressed as

$$\Delta z(\rho) = A e^{-\frac{1}{2}\left(\frac{\rho}{\sigma}\right)^2}, \quad (1)$$

where  $A = 20\mu\text{m}$ ,  $\sigma = 30\text{mm}$  and  $\rho$  is the distance from the support point. The distortion is measured along the normal to the surface. The three support points are located on a ring of radius  $304 \text{mm}$  in the M2C coordinate system giving the following coordinates:

X	Y
304.0 mm	0.0 mm
152.0 mm	263.33 mm
152.0 mm	-263.33 mm

where the X - axis direction is up in the symmetry plane, and the Z-axis is perpendicular to the rim plane away from the aperture.

The resulting surface shape is illustrated in Figure 2-1. Here the distortion is magnified by a factor 2000 to better visualise the distortion distribution across the surface.

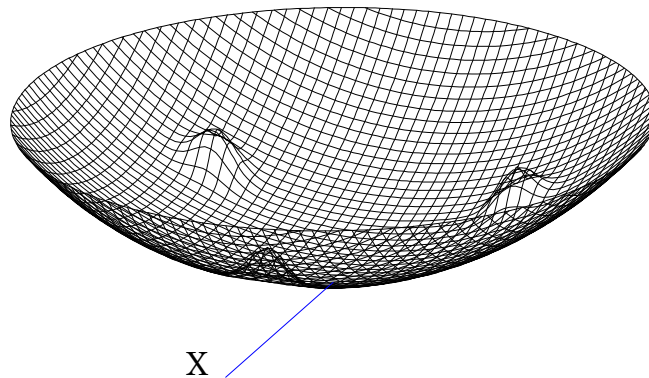


Figure 2-1 Secondary mirror with three Gaussian shaped bumps magnified by a factor 2000.

### 3. RF DEGRADATION FOR 217 GHZ DETECTORS

The RF degradation of the antenna system is calculated with the GRASP8 program at the frequency 217 GHz and for the following four detectors:

Detectors	Position			Pointing direction		
	X [mm]	Y [mm]	Z [mm]	X	Y	Z
_1	-31.180	-27.749	+12.776	.063313	.058579	.996273
_2	-29.527	-8.754	13.236	.060508	.018535	.997996
_5	-16.174	-34.288	9.791	.032614	.072486	.996836
_6	-14.291	-15.164	10.422	.029370	.032199	.999050

Table 2-1 Detector positions and directions in RDP coordinate system

The detector at 217 GHz is modelled as a simple Gaussian tapered feed as defined in the ESA document SCI-PT-RS-07024 with 30 dB taper at 21.8°. The horn pattern is shown in Figure 3-1.

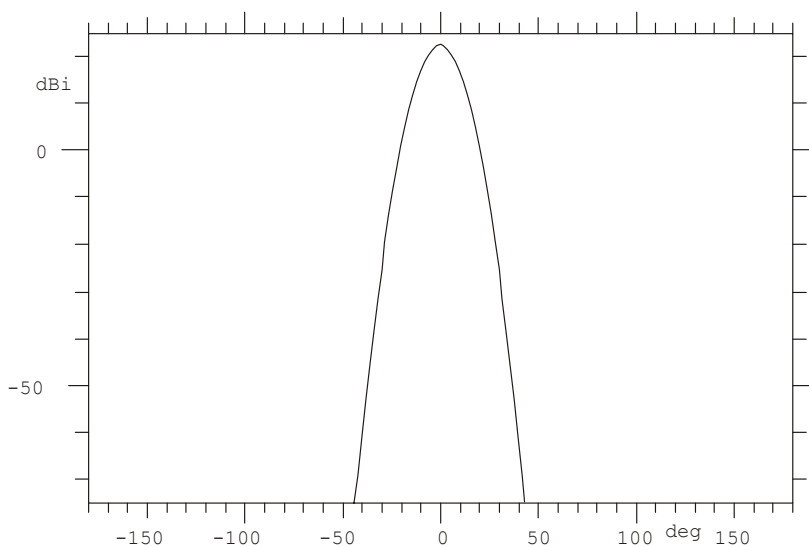


Figure 3-1 Detector HFI\_217 amplitude pattern.

The main beam is calculated using Geometrical Optics, GO, on the secondary mirror and Physical Optics, PO, on the primary mirror. The beams are presented in phi-theta grids around the main beam and in theta cuts through the peak.

### 3.1 HFI\_217\_01

The nominal beam for the HFI\_217\_1 detector is shown in Figure 3-2 in a region of  $.6^\circ$  around the beam maxima.

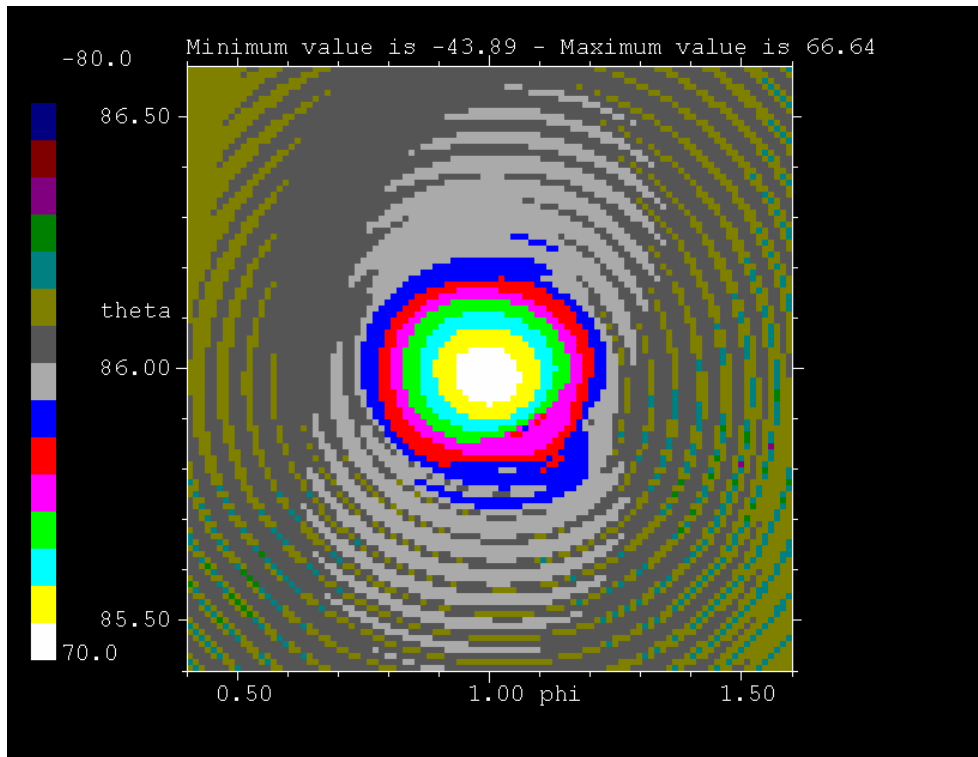


Figure 3-2 Main beam for HFI\_217\_1.

The peak level is found to 66.684 dBi at  $\theta = 85.9857^\circ$  and  $\phi = 0.9954^\circ$ .

The simulated distortions from the three support points give the distorted pattern in Figure 3-3. The pattern is significantly degraded in the sidelobe region. The influence of the surface distortions is more evident in Figure 3-4, where the nominal pattern is subtracted from the distorted pattern. The difference pattern shows a resulting generated broad degradation field with a field maximum of 18.57 dBi.

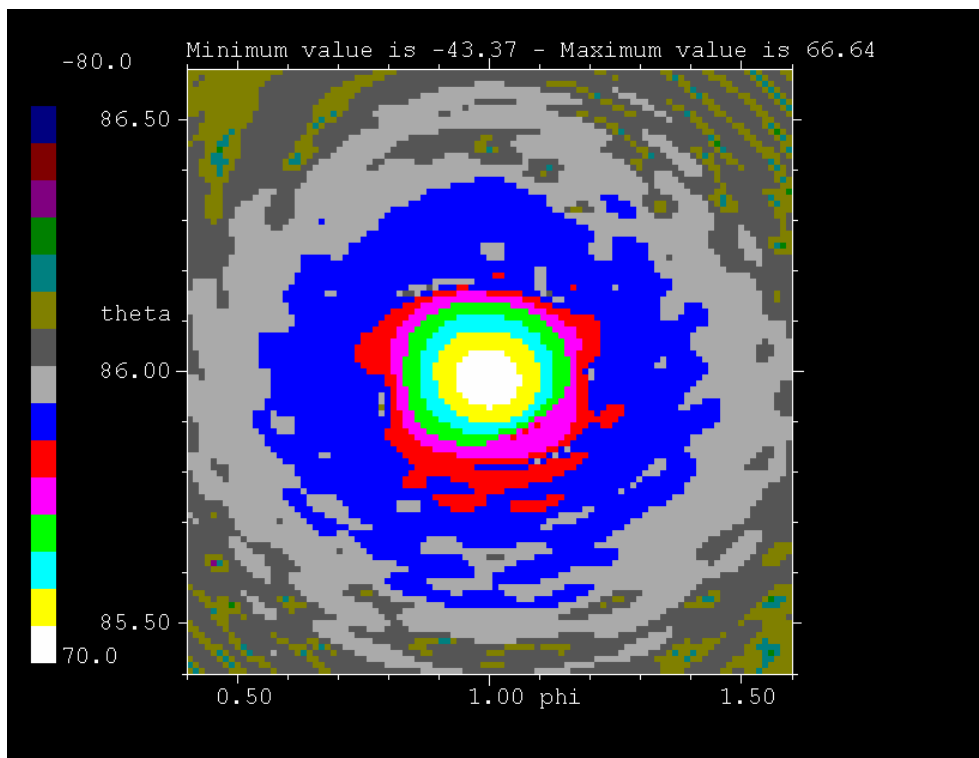


Figure 3-3 Distorted beam for HFI\_217\_1.

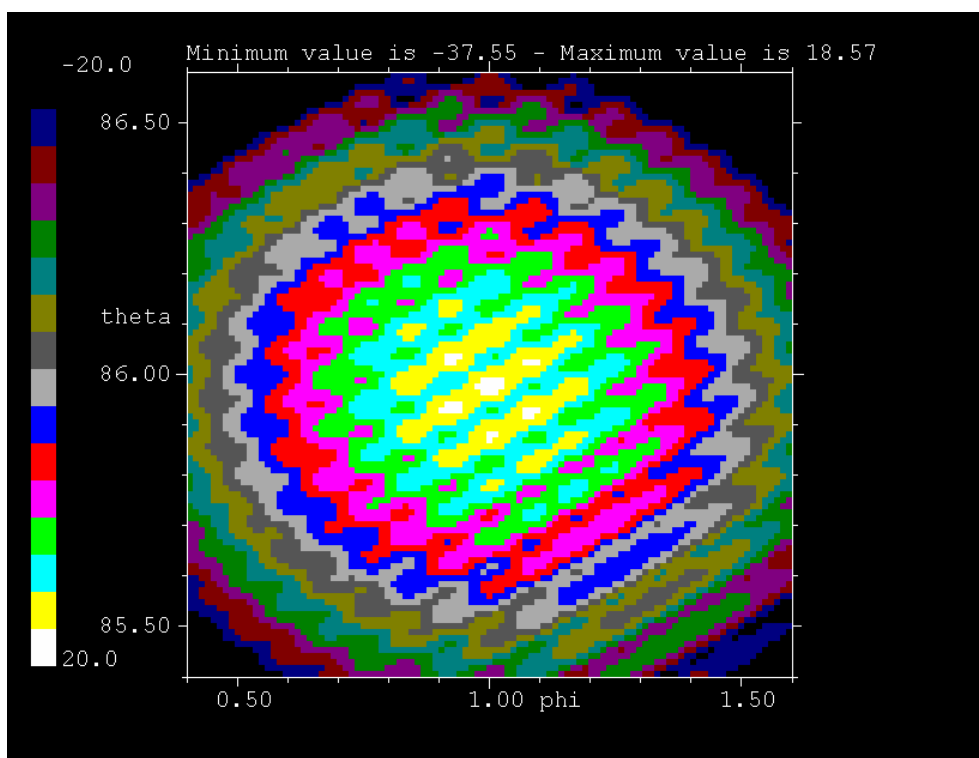


Figure 3-4 Degradation field for HFI\_217\_1.

The pattern cuts through the main beam in Figure 3-5 show the influence of the distortions in more detail.

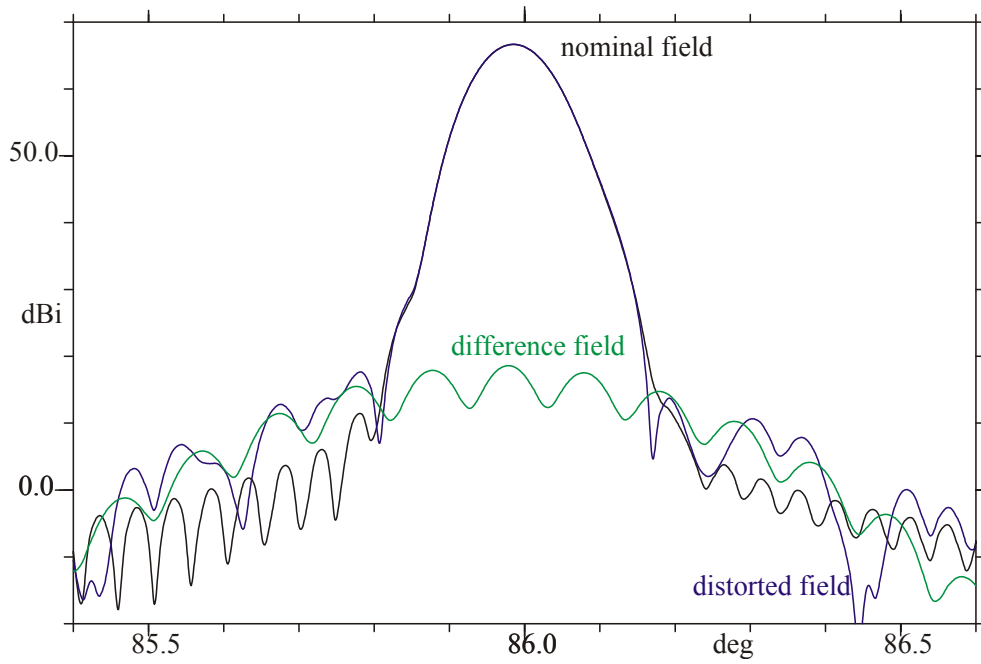


Figure 3-5 Cut through main beam for HFI\_217\_1.

### 3.2 HFI\_217\_02

The nominal beam around the beam maxima for the HFI\_217\_2 detector is shown in Figure 3-6.

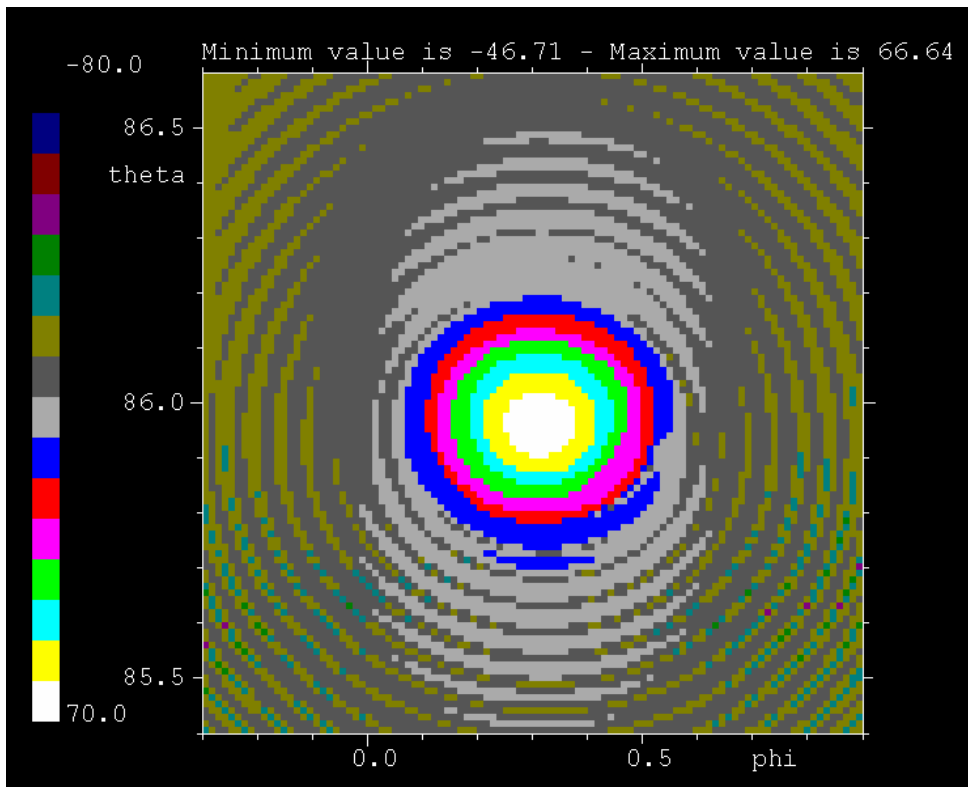


Figure 3-6 Main beam for HFI\_217\_2.

The peak level is found to 66.693 dBi at  $\theta = 85.9592^\circ$  and  $\phi = 0.3146^\circ$ .

The simulated distortions from the three support points give the distorted pattern in Figure 3-7. The difference field, the nominal field subtracted from the distorted field, is shown in Figure 3-8.

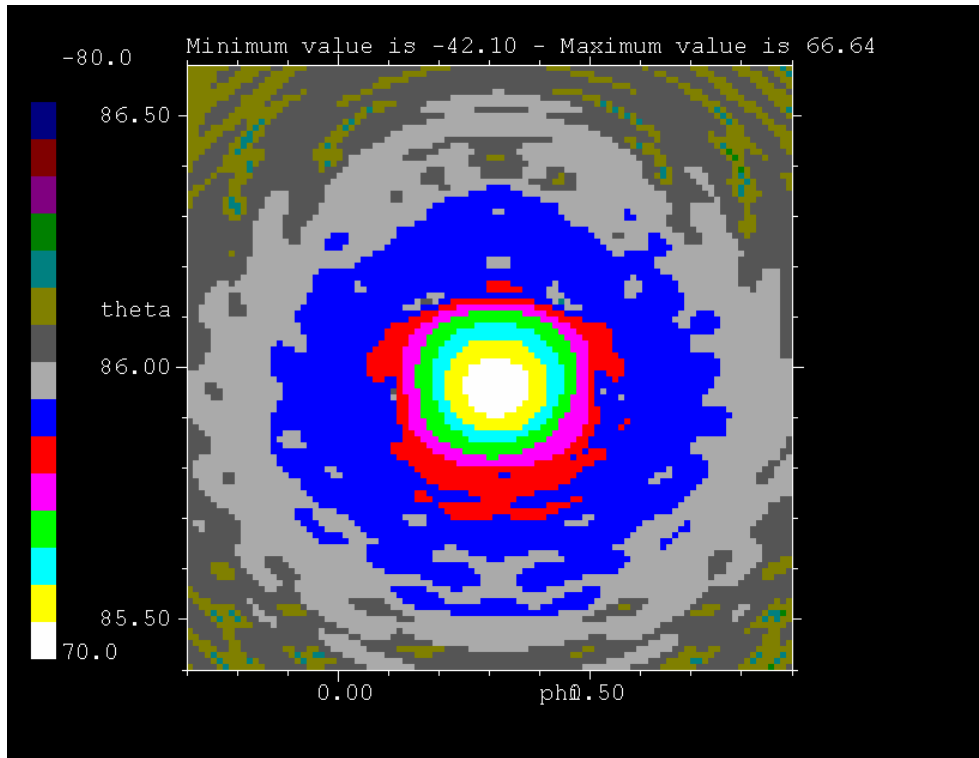


Figure 3-7 Distorted beam for HFI\_217\_2.

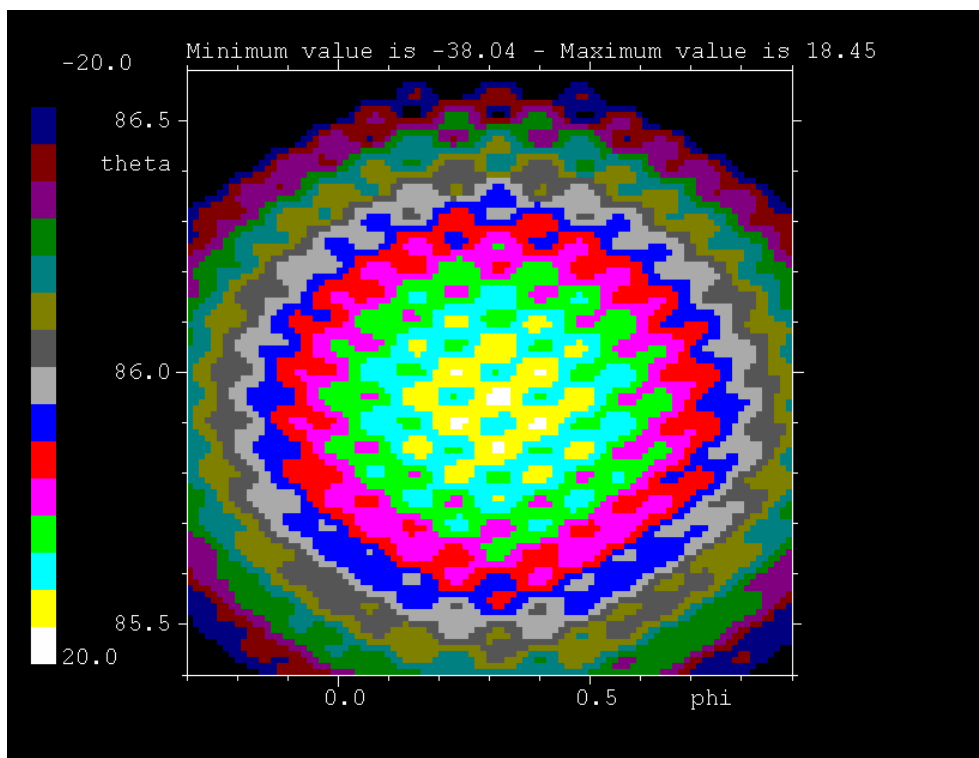


Figure 3-8 Degradation field for HFI\_217\_2.

The pattern cuts through the main beam in Figure 3-9 show the influence of the distortions in more detail.

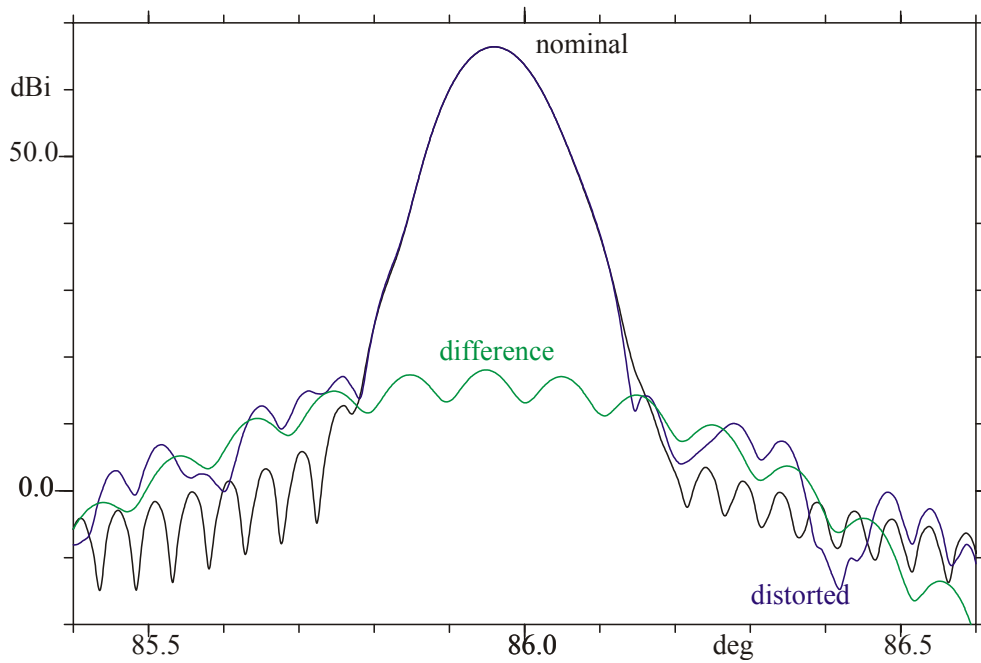


Figure 3-9 Cut through main beam for HFI\_217\_2.

### 3.3 HFI\_217\_05

The nominal beam around the beam maxima for the HFI\_217\_5 detector is shown in Figure 3-10.

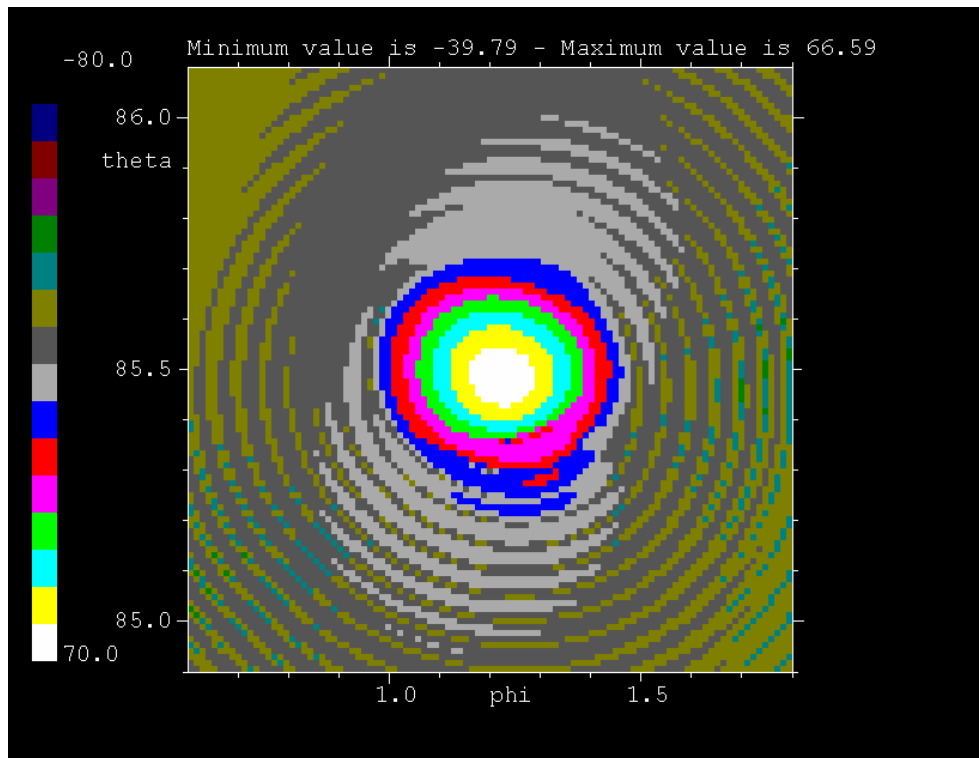


Figure 3-10 Main beam for HFI\_217\_5.

The peak level is found to 66.604 dBi at  $\theta = 85.4852^\circ$  and  $\phi = 1.2251^\circ$ .

The simulated distortions from the three support points give the distorted pattern in Figure 3-11. The difference field, the nominal field subtracted from the distorted field, is shown in Figure 3-12.

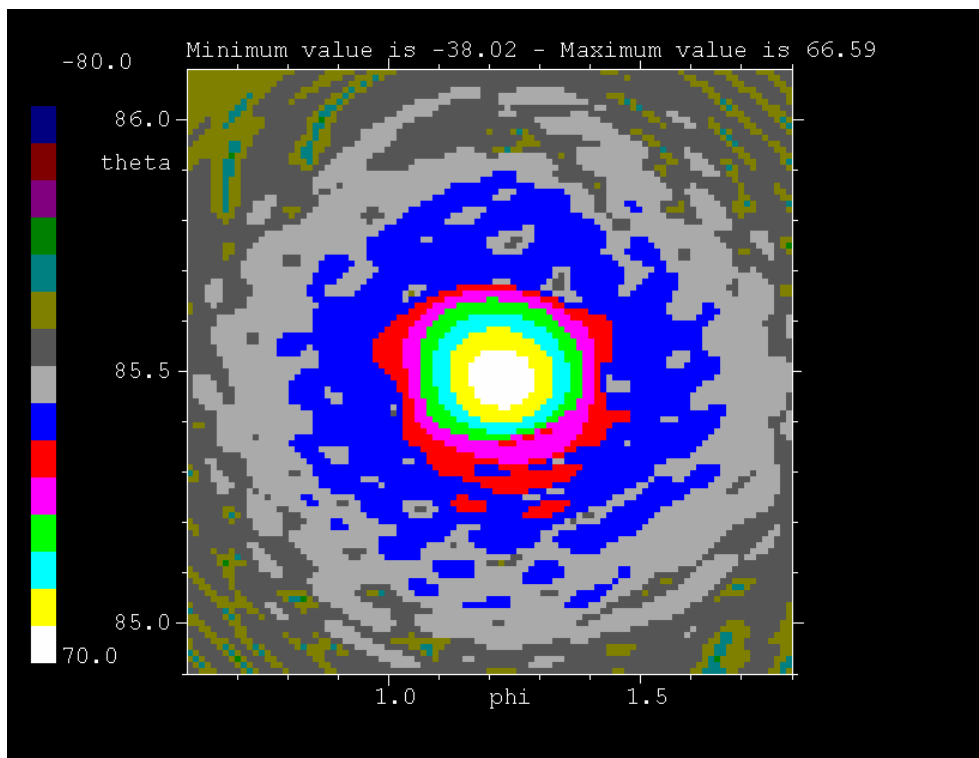


Figure 3-11 Distorted beam for HFI\_217\_5.

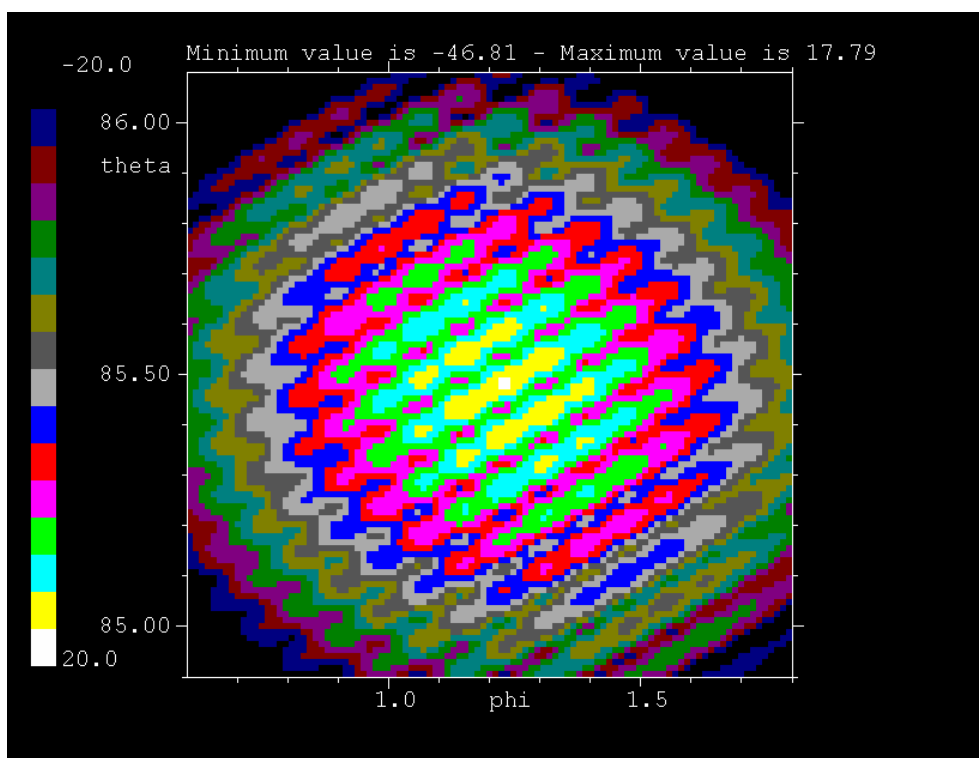


Figure 3-12 Degradation field for HFI\_217\_5.

The pattern cuts through the main beam in Figure 3-13 show the influence of the distortions in more detail.

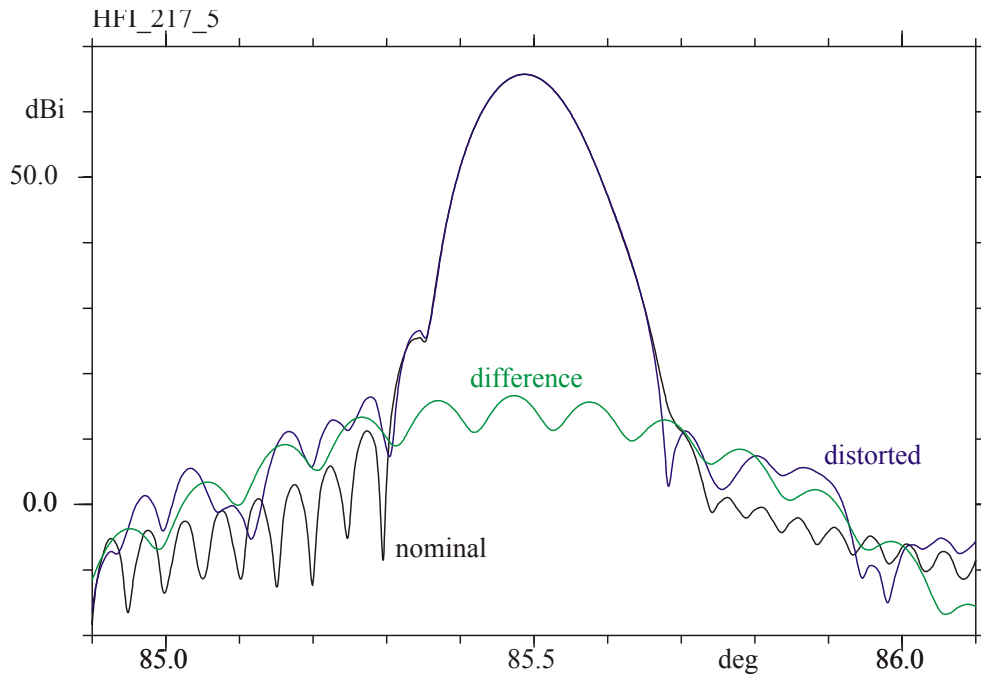


Figure 3-13 Cut through main beam for HFI\_217\_5.

### 3.4 HFI\_217\_06

The nominal beam around the beam maxima for the HFI\_217\_6 detector is shown in Figure 3-14.

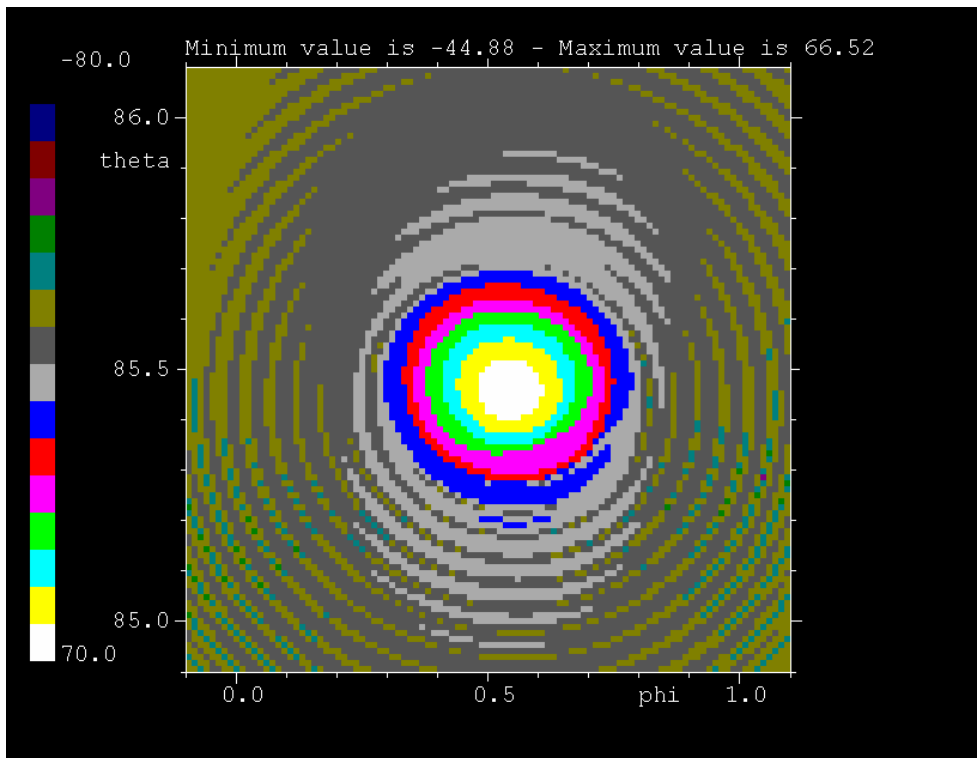


Figure 3-14 Main beam for HFI\_217\_6.

The peak level is found to 66.604 dBi at  $\theta = 85.4581^\circ$  and  $\phi = 0.5435^\circ$ .

The simulated distortions from the three support points give the distorted pattern in Figure 3-15. The difference field, the nominal field subtracted from the distorted field, is shown in Figure 3-16.

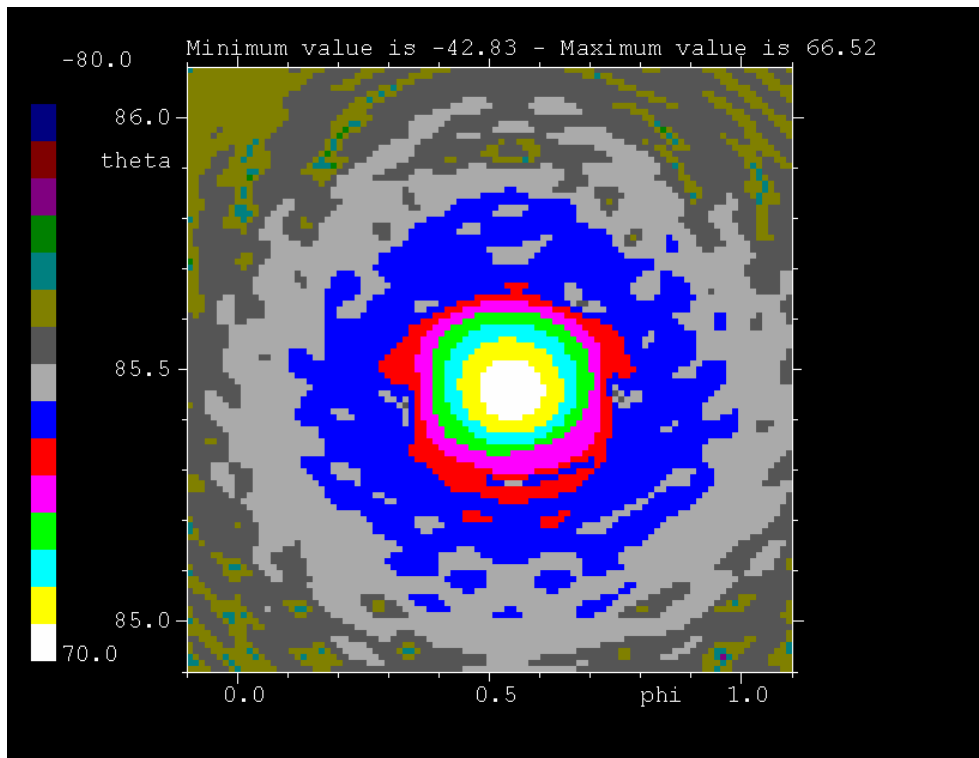


Figure 3-15 Distorted beam for HFI\_217\_6.

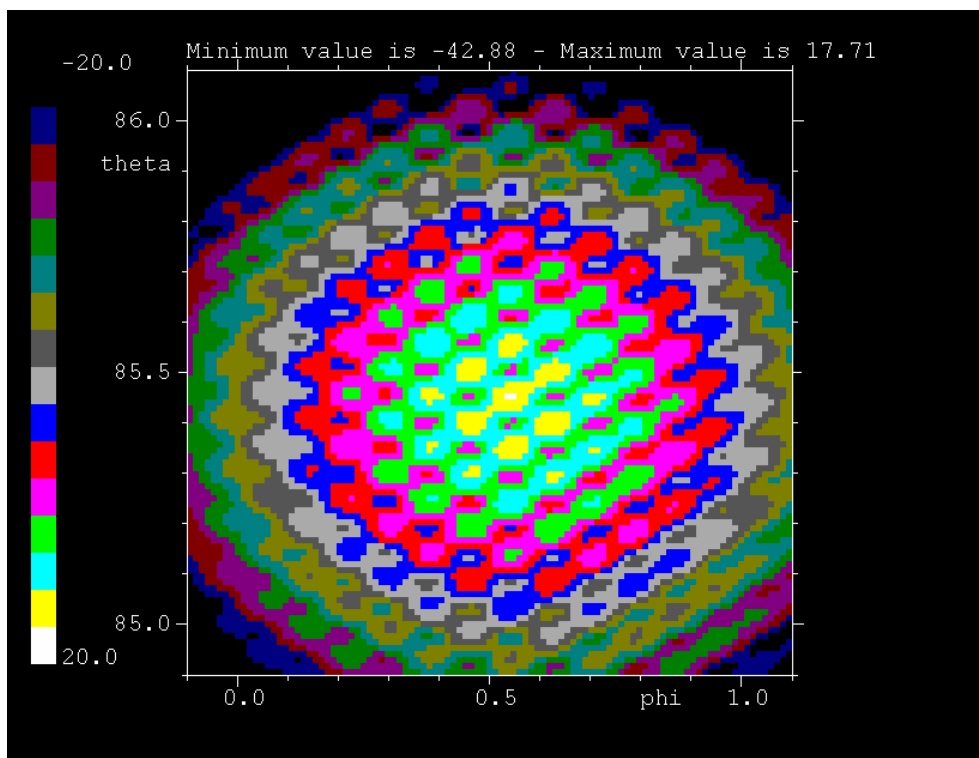


Figure 3-16 Degradation field for HFI\_217\_6.

The pattern cuts through the main beam in Figure 3-17 show the influence of the distortions in more detail.

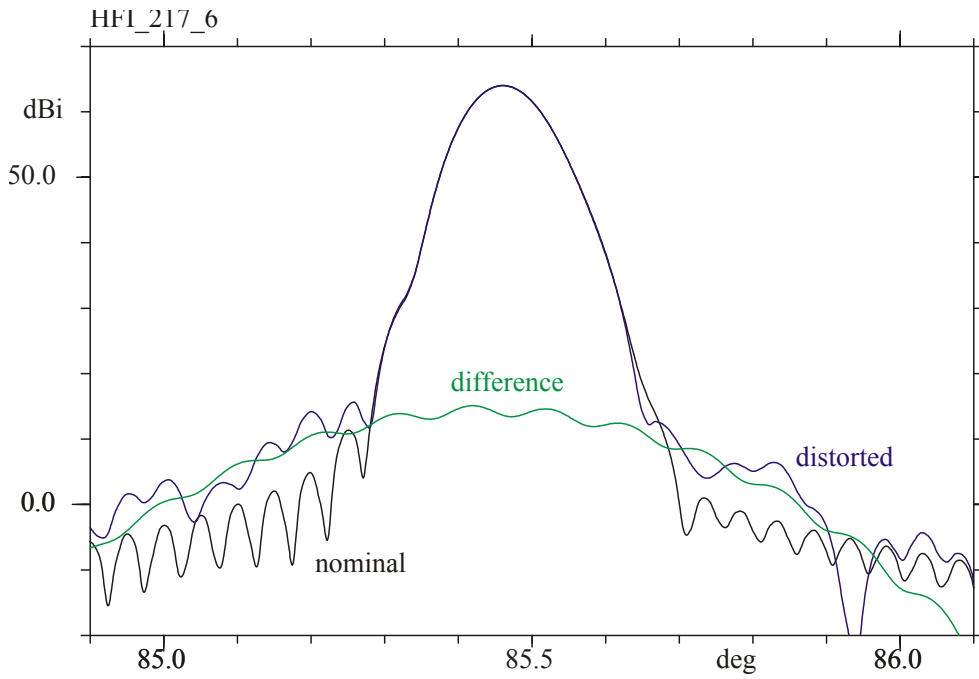


Figure 3-17 Cut through main beam for HFI\_217\_6.

## 4. SCALE INFLUENCE ON PERFORMANCE

In order to detect the influence on the RF performance of the surface distortion size, the distortion pattern is recalculated using the HFI\_217\_01 horn with a peak distortion 3.16 times larger. The resulting difference pattern is shown in Figure 4-1.

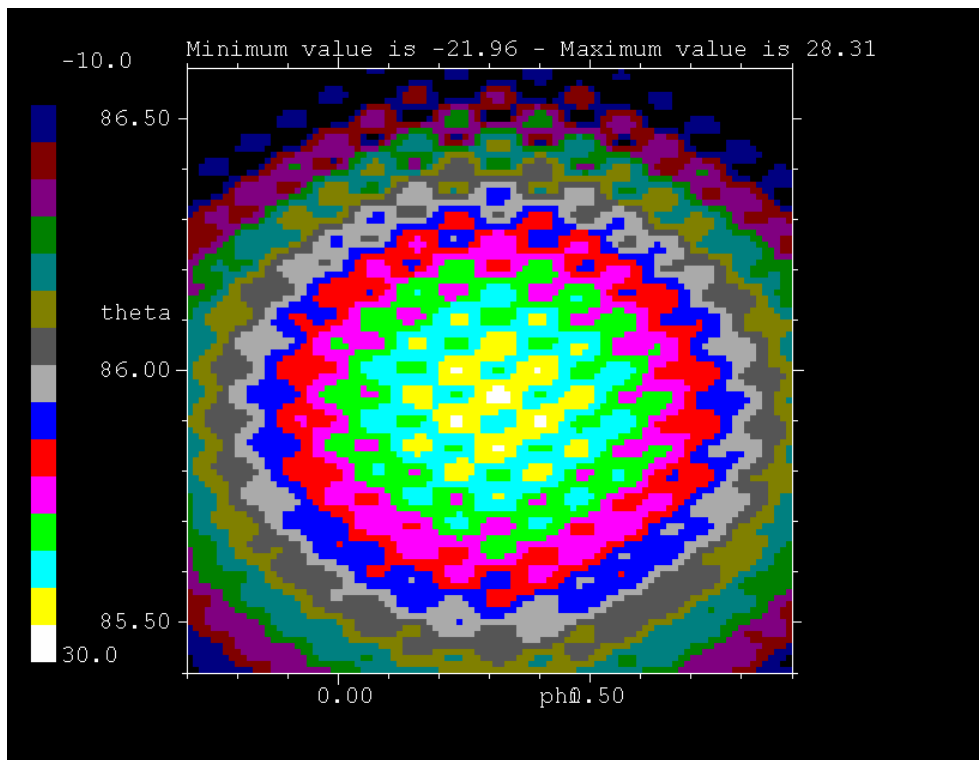


Figure 4-1 Difference beam for enlarged distortions by factor 3.16, HFI\_217\_1.

Compared with Figure 3-4 the patterns are very similar but the level is increased 10 dB. Therefore, the influence on the RF power of the distortions is scalable in a square dependence:  $10 \text{ dB} = 10 \cdot \log[(3.162)^2]$ .

The pattern correlation is also shown in Figure 4-2, where the nominal and the two difference fields for peaks of  $20 \mu\text{m}$  and  $63.256 \mu\text{m}$  are presented in cuts through the main beam.

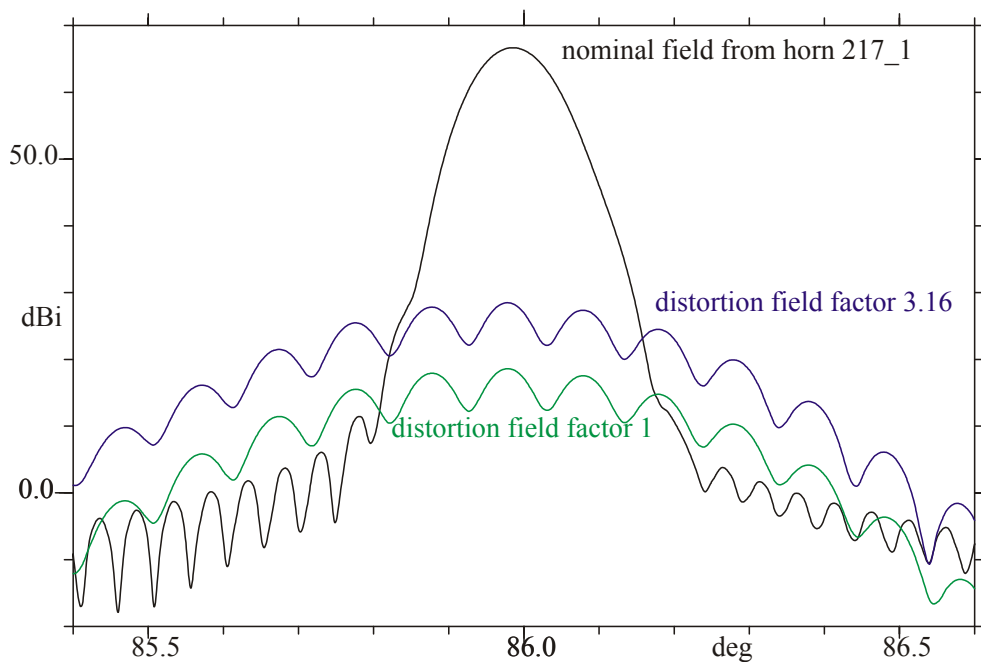


Figure 4-2 Cut through main beam for HFI\_217\_1.

## REFERENCES

ESA (2000)

“Planck Telescope Design Specification”  
SCI-PT-RS-07024, dated 31/08/00.

Alcatel (2001)

“Data interface status”  
Product code 22100,  
H-P-3-ASPI-TN-0096, dated 06/09/01.

Alcatel (2003)

“Planck telescope specification”  
H-P-3-ASPI-SP-0004, dated 17/01/03 – issue: 01-rev 03.